

## Labyrinthine clustering in a spatial rock-paper-scissors ecosystem

Jeppe Juul, Kim Sneppen, and Joachim Mathiesen

*Niels Bohr Institute, University of Copenhagen, Blegdamsvej 17, DK-2100 Copenhagen, Denmark*

(Received 27 September 2012; published 8 April 2013)

The spatial rock-paper-scissors ecosystem, where three species interact cyclically, is a model example of how spatial structure can maintain biodiversity. We here consider such a system for a broad range of interaction rates. When one species grows very slowly, this species and its prey dominate the system by self-organizing into a labyrinthine configuration in which the third species propagates. The cluster size distributions of the two dominating species have heavy tails and the configuration is stabilized through a complex spatial feedback loop. We introduce a statistical measure that quantifies the amount of clustering in the spatial system by comparison with its mean-field approximation. Hereby, we are able to quantitatively explain how the labyrinthine configuration slows down the dynamics and stabilizes the system.

DOI: [10.1103/PhysRevE.87.042702](https://doi.org/10.1103/PhysRevE.87.042702)

PACS number(s): 87.23.Kg, 87.23.Cc, 87.18.Hf

### I. INTRODUCTION

Spatial migration of species is crucial for the viability of many ecological systems. As a striking example, crickets are known to locally deplete their nutritional resources to an extent where mass migration is the only alternative to cannibalism [1,2]. Once the crickets have left an area, they cannot return until the natural resources have been reestablished. Likewise, deadly viruses and bacteria depend on constantly infecting new hosts to survive [3–5].

The rock-paper-scissors game has emerged as a paradigm to describe the impact of spatial structure on biodiversity [6–12]. In this system, three species interact cyclically such that species 1 can invade species 2, which can invade species 3, which, in turn, can invade species 1 [see Fig. 1(a)]. Such an intransitive interaction pattern is very similar to the important genetic regulatory network *the repressilator* [13,14] and has been identified in many ecological systems, among others in marine benthic systems [15,16], plant systems [17–19], terrestrial systems [20,21], and microbial systems [22–26]. In such systems, all species constantly need to migrate spatially to survive, but they may do this at very different speeds. In investigations of three strands of *Escherichia coli* bacteria with cyclic interactions, it has been shown that biodiversity cannot be preserved unless spatial structure is imposed by arranging the bacteria on a Petri dish [6,7,27]. These results have been reproduced in Monte Carlo simulations [28–32], but even though many different analytical approaches have been applied, exactly how spatial structure stabilizes the system is still an open problem [33–35].

### II. MODEL

We study the rock-paper-scissors game on a square lattice of  $L \times L$  nodes and periodic boundary conditions. Each node is occupied by one of the three species 1, 2, or 3 growing at rates  $v_1$ ,  $v_2$ , and  $v_3$ , respectively. In each update a random node  $i$  and a random one of its neighbors  $j$  are selected. If  $i$  can invade  $j$  according to the cyclic interacting pattern illustrated in Fig. 1(a), it will do so with a probability equal to  $v_i$ .

### III. RESULTS

When the three species are initiated from a random configuration and with equal growth rates, they quickly organize into

a steady state where all species are equally abundant and form small clusters [see Fig. 1(b)]. If the growth rate of species 3 is increased compared to species 1 and 2, species 2 becomes more abundant on the lattice and all three species form larger clusters [see Fig. 1(c)]. This paradoxical behavior, that the biomass of one species increases proportionally to the growth rate of its prey, is characteristic for the rock-paper-scissors system [28,29,36].

Similarly, if the growth rate of species 1 is decreased, species 3 slowly becomes scarcer until the system eventually collapses to a state where only the slow species 1 survives [28,37]. The larger the system size is, the smaller  $v_1$  can be while still maintaining biodiversity. Approaching the limit  $v_1 \rightarrow 0$ , a very large lattice is required in order for species 3 to be viable. In this limit an interesting spatial organization is observed. Species 3 propagates through the lattice in thin and broken wave fronts in constant flight from species 2. In the rest of the system the slowly growing species 1 and its prey, species 2, are tangled in a complex configuration with an enormous mutual perimeter. This spatial organization forms an ever-changing labyrinth of narrow pathways in which species 3 propagates [see Figs. 1(d)–1(f)]. The more narrow and twisted the labyrinth becomes, the longer it will take for species 3 to return to a particular location, which gives species 1 more time to grow, forming broader pathways. This complex spatial feedback loop, which is independent of the choice of boundary conditions, stabilizes the configuration, and is destroyed if the species are allowed to diffuse or if a death rate is introduced [38].

Emergence of labyrinthine patterns has previously been observed in magnetic liquids, confined granular-fluid systems, and chemical reaction-diffusion systems [39–41]. In a labyrinthine cluster, points  $i$  and  $j$  that are close to each other in terms of geodesic distance  $d_{\text{geo}}$  are separated by a long distance  $d_{\text{path}}$ , if one is restricted to only travel only along the connected component. To characterize how labyrinthine the spatial organization of a species is, we introduce the local measure

$$\xi_i = \max_{j \in c.c.(i)} \left( \frac{d_{\text{path}}(i, j)}{d_{\text{geo}}(i, j)} \right), \quad (1)$$

with the spatial average  $\xi = \langle \xi_i \rangle$ . Thus,  $\xi_i$  describes how much longer at most one needs to travel along the labyrinth from a

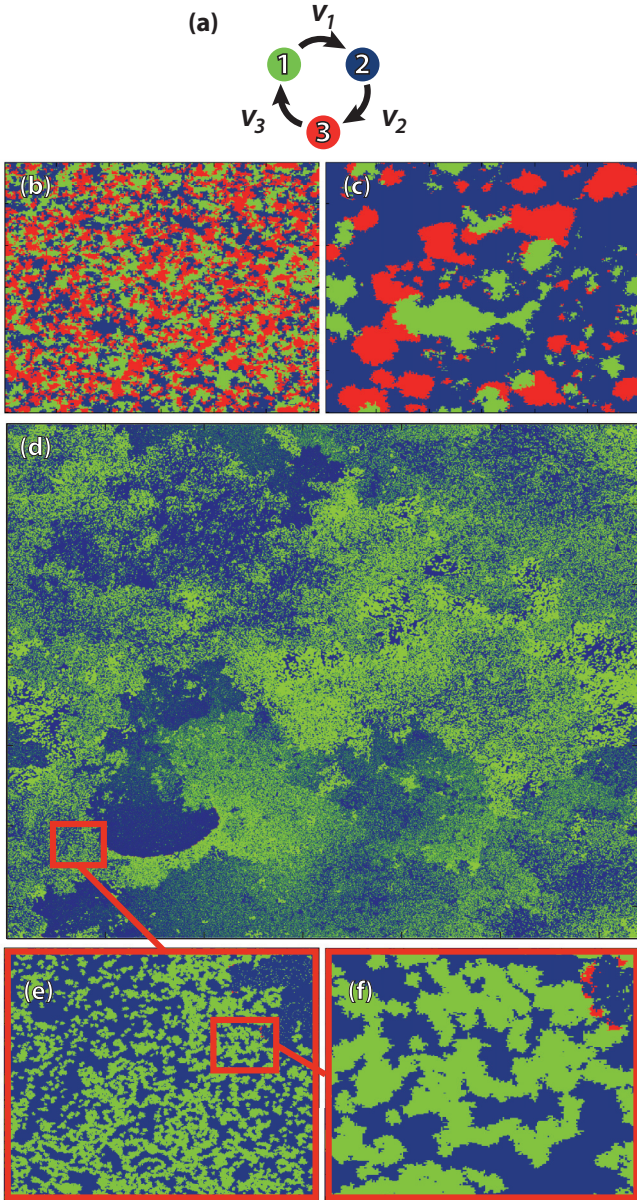


FIG. 1. (Color online) Spatial self-organization in the rock-paper-scissors game. (a) The three species interact cyclically. Species  $i$  invades its prey at rate  $v_i$ . (b)–(d) Snapshots of the steady-state spatial organization of the three species when (b) all species grow at the same rate and  $L = 300$ ; (c) species 3 grows five times faster than 1 and 2 and  $L = 300$ ; (d) species 1 grows 1250 times more slowly than 2 and 3 and  $L = 12\,800$ . (e), (f) Zooms of the system in (d).

point  $i$  to any other point  $j$  in the same connected component, compared to the geodesic distance.  $\xi_i$  pinpoints regions with strong labyrinthine structure, and is found to exhibit huge spatial variations for real labyrinths, critical percolation, or as here for the slow species in a rock-paper-scissor relationship [38]. In Fig. 2(d) it is seen that  $\xi$  of species 1 steadily increases as its growth rate decreases exponentially, confirming that a labyrinthine pattern emerges.

In order to describe the spatial self-organization in steady state, we study the probabilities  $p_1$ ,  $p_2$ , and  $p_3$  of a random node to be occupied by species 1, 2, or 3, respectively.

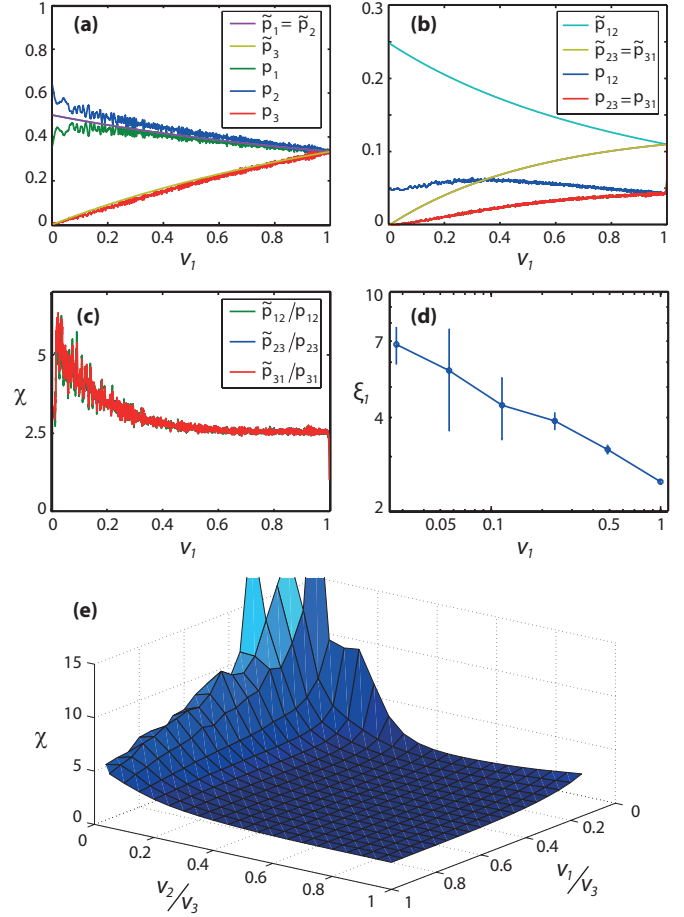


FIG. 2. (Color online) Species abundances and correlations for small  $v_1$ . (a) When the growth rate of species 1 is decreased, species 3 becomes less abundant. The mean-field theory provides a good approximation to the abundances. (b) The spatial correlation between different species are much lower than predicted by the mean-field theory due to clustering. (c) The ratio between the predicted mean-field correlations and the observed correlations are equal for all species. This ratio defines  $\chi$ . (d) When the growth rate of species 1 is decreased, it begins to form labyrinthine clusters. Thus, the path distance between two points  $i$  and  $j$  in the same cluster becomes much longer than the geodesic distance. This ratio is described by  $\xi$ . (e) When  $v_3 \gg v_1, v_2$ , the ratio  $\chi$  diverges corresponding to the large clustering in Fig. 1(c). When one species grows much more slowly than the others,  $\chi$  approaches 5, which gives rise to the labyrinthine clustering in Fig. 1(d).

Furthermore, we are interested in the spatial correlations  $p_{ij}$  between species  $i$  and  $j$ . That is, the probability of a random node and a random one of its neighbors to be occupied by species  $i$  and  $j$ , respectively.

Given these correlations the time evolution of species abundances is given by [33]

$$\dot{p}_1 = v_1 p_{12} - v_3 p_{31}, \quad (2)$$

where the equations for  $\dot{p}_2$  and  $\dot{p}_3$  follow by cyclic permutation of the indices 1, 2, and 3. This symmetry also holds for all subsequent equations of this article.

In the mean-field approximation, all nodes are linked and spatial structure does not exist. Then the correlation

between two species is simply given by the product of species abundances  $\tilde{p}_{12} = \tilde{p}_1 \tilde{p}_2$ , where the tilde ( $\sim$ ) denotes that the mean-field approximation has been applied. If this is inserted into (2) and the time derivatives are set to zero, one obtains the steady-state solution

$$\tilde{p}_1 = \frac{v_2}{v_1 + v_2 + v_3}, \quad (3)$$

$$\tilde{p}_{12} = \frac{v_2 v_3}{(v_1 + v_2 + v_3)^2}. \quad (4)$$

In Figs. 2(a) and 2(b) the steady-state abundances and correlations are shown at constant  $v_2 = v_3 = 1$  and varying  $v_1 \leq 1$ . It is seen that a slow growth rate of species 1 leads to a decline in the abundance of species 3. Mean-field theory provides a good approximation for how abundances depend on growth rates, with the only slight deviation that species 2 becomes slightly more abundant than species 1 for low  $v_1$ . However, the mean-field approach cannot capture the spatial organization of the species, and thus it predicts interspecies correlations far larger than those observed in simulations [see Fig. 2(b)]. The fact that the abundances are correctly predicted indicates that the mean-field correlations are proportional to the true, spatial correlations. Indeed, if (2) is set to zero for both the spatial and mean-field systems one can derive the relations

$$\frac{\tilde{p}_{12}}{p_{12}} = \frac{\tilde{p}_{23}}{p_{23}} = \frac{\tilde{p}_{31}}{p_{31}} \equiv \chi. \quad (5)$$

Here we have introduced the ratio  $\chi$ , defined by how much the time average of the correlations between two species is larger in the steady state of the mean-field approximation compared to the spatial system [see Fig. 2(c)]. This statistical measure describes the spatial and dynamical organization of the rock-paper-scissors game for varying growth rates. The intuition behind  $\chi$  is the following.

The average time before a node of species 2 is invaded by species 1 is given by  $T_1 = \frac{p_2}{v_1 p_{12}}$  for the spatial system and  $\tilde{T}_1 = \frac{\tilde{p}_2}{v_1 \tilde{p}_{12}}$  in mean field. Therefore,  $\chi \approx \frac{T_1}{\tilde{T}_1}$  provides a measure for how much longer each species on average lives on a node before being invaded, compared to the result in the mean-field system, i.e., how much the spatial organization slows down the dynamics. Furthermore, when  $\chi$  is large the correlations of the spatial system are much smaller than in the mean-field system, according to (5), so the species must have a high degree of clustering. Hence,  $\chi$  gives a measure for the clustering of the spatial system. These two interpretations are, of course, tightly connected. If the average cluster diameters are doubled, each node will live for twice as long before being invaded, corresponding to increasing  $\chi$  by a factor of 2.

How does  $\chi$  depend on the growth rates of the three species? In Fig. 2(e) this dependency is shown as a function of the relative growth rates  $\frac{v_1}{v_3}$  and  $\frac{v_2}{v_3}$ , with  $v_3$  chosen to be the fastest-growing species. When all growth rates are equal we have  $\chi \approx 2.5$ , corresponding to the moderate amount of clustering observed in Fig. 1(b). When species 3 grows much faster than the two other species, such that both growth ratios go to zero,  $\chi$  becomes very large. This agrees well with the large amount of clustering observed in Fig. 1(c).

When only  $v_1 \rightarrow 0$  we see from Figs. 1(d) and 2(d) that  $\chi$  approaches a finite value close to 5. In this limit, we expect

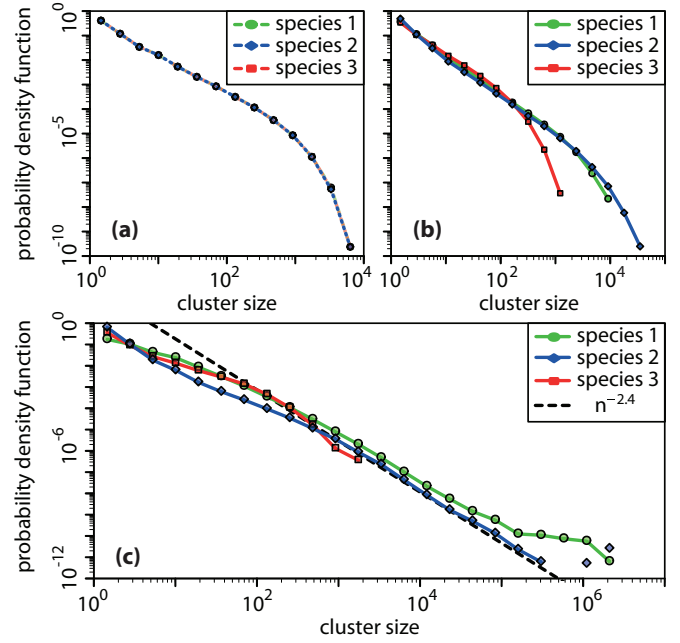


FIG. 3. (Color online) Cluster size distributions. (a) When all species grow at the same rate, all clusters consist of fewer than 5000 nodes. Here  $v_1 = v_2 = v_3 = 1$ . (b) When the growth rate of species 1 is decreased, species 3 becomes less abundant and large clusters of species 1 and 2 become more likely. Here  $v_1 \approx 0.5$  and  $v_2 = v_3 = 1$ . (c) In the limit  $v_1 \rightarrow 0$  the cluster size distributions of species 1 and 2 become heavy tailed with a cutoff set by the system size. Here  $v_1 \leq 0.007$  and  $v_2 = v_3 = 1$ . For all plots  $L = 2048$ .

from (3) that  $p_3 \rightarrow 0$  while  $p_1 \approx p_2 \rightarrow \frac{1}{2}$ . In this case, the amount of clustering of species 3 is limited. The observation of  $\chi$  suggests that clustering reduces the spatial correlation between species 2 and 3 by only a factor of 5 compared to the mean-field system. This sets an upper bound for how much species 1 and 2 can cluster. The mean-field approach predicts a correlation of  $\tilde{p}_{12} = \frac{1}{4}$ , so with  $\chi \approx 5$  Eq. (5) dictates the spatial correlation to be  $p_{12} \approx \frac{1}{20}$ . This agrees well with the  $12\,800 \times 12\,800$  system in Fig. 1(d), where  $v_1 = 0.0008$ ,  $v_2 = v_3 = 1$ , and  $p_{12} \approx 0.05$ , which is also evident from Fig. 2(b).

While the value of  $\chi$  quantifies the average amount of clustering, it does not provide information on the cluster size distribution. In the case where all species grow the same rate, Fig. 1(b) suggests that clusters have a characteristic size. Indeed, Fig. 3 shows that the cluster size distribution in this case sharply decreases for clusters larger than 1000 nodes. When the growth rate of species 1 goes to zero, however, species 3 continues to be organized in small clusters, but large clusters of species 1 and 2 become much more likely. The cluster size distributions of these become exceedingly broad, culminating in a heavy tail distribution with a cutoff that is set by the system size.

An alternative approach that has been applied to describe the spatial organization of the rock-paper-scissors game is the pair approximation [34,42]. This approximation predicts  $\chi = 1.5$ , which is far from the observed value of  $\chi = 2.5$ , further illustrating the inability of the pair approximation to describe the behavior of the rock-paper-scissors game.

## IV. DISCUSSION

Our results quantitatively describe how spatial clustering slows down the dynamics of the rock-paper-scissors game, and why this leads to a labyrinthine spatial organization in the limit where one species grows slowly compared to the two others: an organization that includes a type of excitable front that propagates on self-organized labyrinthine clusters distributed over many length scales. In this limit of one slow species, the largest clusters of both the slow species and its prey cover a large fraction of the system, as seen in Fig. 2(d). This consequence of the labyrinthine configuration would not be possible in site percolation, where each of the large species would need to occupy close to 60% of the nodes to percolate [43].

Interestingly, the extreme version of the rock-paper-scissors ecology with one slow species resembles the forest fire model

in a fire-tree-ashes analogy [44–46]. The slow species would then be forest, which is burned by fire, which is replaced by ashes, from which trees can again slowly grow. The main differences from existing forest fire models are that in the present system trees can grow only in the neighborhood of other trees and fire can be extinguished only in the neighborhood of ashes.

The method of quantifying how much clustering slows down the dynamics of a spatial system, compared to the mean-field approximation, is quite general, and we expect it to be applicable on a broad range of dynamical systems. In particular, it may be useful in predicting the spatial organization in predator-prey models, which continues to attract much attention within the field of complex systems [47,48].

- 
- [1] S. Simpson, G. Sword, P. Lorch, and I. Couzin, *Proc. Natl. Acad. Sci. USA* **103**, 4152 (2006).
- [2] G. Sword, P. Lorch, and D. Gwynne, *Nature (London)* **433**, 703 (2005).
- [3] D. Morens, G. Folkers, and A. Fauci, *Nature (London)* **430**, 242 (2004).
- [4] K. Sneppen, A. Trusina, M. H. Jensen, and S. Bornholdt, *PLoS One* **5**, e13326 (2010).
- [5] J. Juul and K. Sneppen, *Phys. Rev. E* **84**, 036119 (2011).
- [6] B. Kerr, M. A. Riley, M. W. Feldman, and B. J. M. Bohannan, *Nature (London)* **418**, 171 (2002).
- [7] T. Reichenbach, M. Mobilia, and E. Frey, *Nature (London)* **448**, 1046 (2007).
- [8] G. Szabó and G. Fáth, *Phys. Rep.* **446**, 97 (2007).
- [9] L. Jiang, T. Zhou, M. Perc, X. Huang, and B. Wang, *New J. Phys.* **11**, 103001 (2009).
- [10] E. Frey, *Physica A* **389**, 4265 (2010).
- [11] L. Jiang, T. Zhou, M. Perc, and B. Wang, *Phys. Rev. E* **84**, 021912 (2011).
- [12] P. P. Avelino, D. Bazeia, L. Losano, J. Menezes, and B. F. Oliveira, *Phys. Rev. E* **86**, 036112 (2012).
- [13] M. Elowitz and S. Leibler, *Nature (London)* **403**, 335 (2000).
- [14] M. Elowitz, A. Levine, E. Siggia, and P. Swain, *Science Signaling* **297**, 1183 (2002).
- [15] J. Jackson and L. Buss, *Proc. Natl. Acad. Sci. USA* **72**, 5160 (1975).
- [16] K. Sibly, *Ecol. Monographs* **56**, 73 (1986).
- [17] D. D. Cameron, A. White, and J. Antonovics, *J. Ecol.* **97**, 1311 (2009).
- [18] R. A. Lankau and S. Y. Strauss, *Science* **317**, 1561 (2007).
- [19] D. R. Taylor and L. W. Aarssen, *Am. Nat.* **136**, 305 (1990).
- [20] B. Sinervo and C. Lively, *Nature (London)* **380**, 240 (1996).
- [21] T. R. Birkhead, N. Chaline, J. D. Biggins, T. Burke, and T. Pizzari, *Evolution* **58**, 416 (2004).
- [22] R. Durrett and S. Levin, *J. Theor. Biol.* **185**, 165 (1997).
- [23] J. Nahum, B. Harding, and B. Kerr, *Proc. Natl. Acad. Sci. USA* **108**, 10831 (2011).
- [24] B. Kirkup and M. Riley, *Nature (London)* **428**, 412 (2004).
- [25] M. E. Hibbing, C. Fuqua, M. R. Parsek, and S. B. Peterson, *Nat. Rev. Microbiol.* **8**, 15 (2010).
- [26] P. Trosvik, K. Rudi, K. O. Strætkvern, K. S. Jakobsen, T. Næs, and N. Chr. Stenseth, *Environ. Microbiol.* **12**, 2677 (2010).
- [27] B. Kerr, C. Neuhauser, B. J. M. Bohannan, and A. M. Dean, *Nature (London)* **442**, 75 (2006).
- [28] M. Frean and E. R. Abraham, *Proc. R. Soc. London, Ser. B* **268**, 1323 (2001).
- [29] C. R. Johnson and I. Seinen, *Proc. Biol. Sci.* **269**, 655 (2002).
- [30] M. Berr, T. Reichenbach, M. Schottenloher, and E. Frey, *Phys. Rev. Lett.* **102**, 048102 (2009).
- [31] J. Mathiesen, N. Mitarai, K. Sneppen, and A. Trusina, *Phys. Rev. Lett.* **107**, 188101 (2011).
- [32] Q. He, M. Mobilia, and U. C. Täuber, *Phys. Rev. E* **82**, 051909 (2010).
- [33] T. Reichenbach, M. Mobilia, and E. Frey, *Phys. Rev. E* **74**, 051907 (2006).
- [34] G. Szabó, A. Szolnoki, and R. Izsák, *J. Phys. A* **37**, 2599 (2004).
- [35] A. Dobrinevski and E. Frey, *Phys. Rev. E* **85**, 051903 (2012).
- [36] Q. He, U. C. Täuber, and R. K. Zia, *Eur. Phys. J. B* **85**, 141 (2012).
- [37] J. Juul, K. Sneppen, and J. Mathiesen, *Phys. Rev. E* **85**, 061924 (2012).
- [38] See Supplemental Material at <http://link.aps.org/supplemental/10.1103/PhysRevE.87.042702> for further details on the species mobility, species mortality, and boundary conditions, and the application of the measure  $\xi$  to different labyrinthine systems.
- [39] R. Rosensweig, *Ferrohydrodynamics*, Dover Books on Physics (Dover, New York, 1997).
- [40] B. Sandnes, H. A. Knudsen, K. J. Måløy, and E. G. Flekkøy, *Phys. Rev. Lett.* **99**, 038001 (2007).
- [41] K. Lee, W. McCormick, Q. Ouyang, and H. Swinney, *Science* **261**, 192 (1993).
- [42] K. Tainaka, *Phys. Lett. A* **176**, 303 (1993).
- [43] D. Stauffer and A. Aharony, *Introduction to Percolation Theory* (Taylor & Francis, London, 1992).
- [44] P. Bak, K. Chen, and C. Tang, *Phys. Lett. A* **147**, 297 (1990).
- [45] B. Drossel and F. Schwabl, *Phys. Rev. Lett.* **69**, 1629 (1992).
- [46] K. Christensen, H. Flyvbjerg, and Z. Olami, *Phys. Rev. Lett.* **71**, 2737 (1993).
- [47] C. A. Lugo and A. J. McKane, *Phys. Rev. E* **78**, 051911 (2008).
- [48] D. Vasseur and J. Fox, *Nature (London)* **460**, 1007 (2009).